# Surface-Enhanced Raman Scattering Studies of Human Transcriptional Coactivator p300

**G. V. Pavan Kumar,[†] B. A. Ashok Reddy,[‡] Mohammed Arif,[‡] Tapas K. Kundu,[‡] and Chandrabhas Narayana*[,†]**

*Light Scattering Laboratory, Chemistry and Physics of Materials Unit, and Transcription and Disease Laboratory, Molecular Biology and Genetics Unit, Jawaharlal Nehru Centre for Advanced Scientific Research, Jakkur P.O., Bangalore 560064, India*

*Received: May 19, 2006*

We report for the first time the surface-enhanced Raman scattering (SERS) studies on p300, a large multidomain transcriptional coactivator protein. Vibration spectral analysis has been performed in an attempt to understand the structure of the p300 in the absence of its crystal structure. Strong Raman bands associated with amides I−III have been observed in the protein spectra. This has been confirmed by performing SERS on deuterated p300. We also observe Raman bands associated with the α-helix, tryptophan, phenylalanine, tyrosine, and histidine. These bands will provide an ideal tool to study the drug−protein interactions in therapeutics using SERS. We have successfully demonstrated the chloride ion effect on the SERS of p300. The Raman intensity increases in the SERS spectra upon addition of chloride ion along with appearance of new modes. We have developed a new method, namely, the "sandwich technique", which could be used to perform SERS experiments on proteins in dry conditions.

## Introduction

p300 was originally identified using protein−interaction assays with the adenoviral E1A oncoprotein.[1] It has been implicated in a number of diverse biological functions including proliferation, cell cycle regulation, apoptosis, differentiation, and DNA damage response.[2−5] Primarily p300 functions as transcriptional coactivator for a number of nuclear proteins. These include known oncoproteins (e.g., myb, jun, fos), transforming viral proteins (e.g., E1A, E6, and large T antigen), and tumor suppressor proteins (e.g., p53, E2F, Rb, and BRCA1).[6] p300 protein is endowed with histone acetyltransferase (HAT) activity.[7,8] Apart from the histones, p300 also acetylates several non-histone proteins with functional consequences.[9] Recently, it has been shown that the non-histone substrate of p300 also includes histone chaperone NPM 1, which activates the chromatin-mediated transcription in an acetylation-dependent manner.[10] Due to its diverse functional importance any alteration of the function of p300 leads to several diseases, which include cancer, diabetes, Rubinstein−Taybi syndrome, etc.[6,9,11] Therefore, p300 is a novel target for therapeutics.

Although extensive work has been done to understand the functional mechanisms of such an important transcriptional coactivator the exact structure−function relations of p300 are yet to be established. Raman spectroscopy has been used in the past to get important structural information from various biological systems, like proteins, nucleotides, peptides, etc. Large concentrations of these biological systems are a must to do routine Raman experiments. In the case of proteins, polypeptides, and nucleotides it is commonly observed that routine Raman fails, due to lack of large concentrations, huge fluorescence, or very weak signals. In the case of p300, as discussed later, it is nearly impossible to get any normal Raman spectra. But, upon addition of some silver nanoparticles to the aqueous solution of the p300, a large enhancement in Raman intensities has been observed, which is due to the surface-enhanced Raman scattering (SERS) phenomenon.

Ever since its discovery,[12] SERS has emerged as an effective tool to study molecules of biological interest.[13] The Raman signal intensity of a molecule gets enhanced by many orders of magnitude ($\sim 10^{6-}10^{8}$) upon adsorption to metal surfaces exhibiting atomic-scale roughness.[14] This phenomenon has been used as an effective detection tool to probe different aspects of biology.[15−17] In recent years, there is a growing interest in studying vibration spectra of amino acids[18] and proteins[19,20] in solution phase at very low concentrations using the SERS technique because of its possible detection capabilities. SERS has also been used to study protein−drug interactions,[21] DNA−molecule interactions,[22,23] etc., with a significant amount of success.

In this paper, we report the SERS experiments carried out on p300 and present the complete vibration spectral analysis, which throws light into the full length 300 kDa protein structure. In the vibrational spectra, it is possible to identify modes related to various functional groups of the protein, which would provide a key to understanding the protein−drug interactions. In addition to this, we have also studied the effect of chloride ion on the SERS of p300 protein. Chloride ion provides a better aggregation of silver nanoparticles around the molecule resulting in large enhancement in Raman signals. This is observed in the case of p300 also. To make a comparative study of the effect of silver nanoparticles on aqueous and dry samples of p300, we have performed SERS on p300 dried on a glass substrate in the presence of silver nanoparticles, and the results are reported here.

## Experimental Details

**Expression and Purification of Full-Length Recombinant Human p300 and Purification of Human (HeLa) Core Histones.** The full-length p300 was purified from the recom-

* Corresponding author. E-mail: cbhas@jncasr.ac.in.
[†] Chemistry and Physics of Materials Unit.
[‡] Molecular Biology and Genetics Unit.

10.1021/jp063071e CCC: $33.50 
Published on Web 08/03/2006

binant bacculovirus-infected Sf-21 cells as a $His_6$-tagged protein through the nickel−nitrilotriacetic acid affinity column (Qiagen) as described in ref 10. The protein was dialyzed against BC100 (20 mM Tris−HCl (pH 7.9), 10% glycerol, 0.2 mM EDTA (pH 8.0), 100 mM NaCl, 0.5 mM PMSF, 0.01 M 2-mercaptoethonol, and 0.1% NP40) to remove the imidazole for doing the SERS experiments. To deuterate the protein, p300 was incubated in $D_2O$ before performing the SERS experiments. The nanoparticles in $D_2O$ solution were used for the deuterated protein experiments. Human core histones used as substrates in the acetyltransferase assays were purified from HeLa nuclear pellet as described in ref 10. Protein concentrations were used as mentioned in the figure legends.

**Histone Acetyltransferase (HAT) Assay.** HAT activity of p300 was performed as described in ref 24. In brief, the indicated amounts of highly purified human core histones were incubated in HAT assay buffer containing 50 mM Tris−HCl, pH 8.0, 10% (v/v) glycerol, 1 mM dithiothreitol, 1 mM phenyl methyl sulfonyl fluoride, 0.1 mM EDTA, pH 8.0, 10 mM sodium butyrate, and 1 $\mu$L of 3.3 Ci/mmol [$^3$H]acetyl coenzyme A (acetyl-CoA) (Perkin-Elmer-NEN) at 30 °C for 30 min. The final reaction volume was 30 $\mu$L. The reaction was stopped by incubating the mixture on ice for 10 min before blotting onto P-81 (Whatman) filter papers. The radioactive counts were recorded on a Wallac 1409 liquid scintillation counter. To visualize the radiolabeled acetylated histones, the reaction mixtures were resolved on 15% SDS−polyacrylamide gel and processed for fluorography as described in ref 25.

**Raman Spectroscopy.** The Raman excitation light (632.8 nm), provided by a He−Ne laser (model 25-LHR-151-230, Melles-Griot, U.S.A.), traversed a band-pass filter (XL12-633NB4, Omega Optical Inc., U.S.A.) and was launched into an epi-illuminated microscope (Nikon 50i, Nikon, Japan; axial resolution ~1 $\mu$m) for micro-Raman experiments. The microscope objective both focused the excitation light and collected the Raman-scattered light in a backscattering geometry. A dichroic beam splitter (660DCLP, Chroma Technology Corp.) redirected the Raman-scattered light from the microscope to a 100 $\mu$m single-core, multimode optical fiber atop the microscope. The light passed through an edge filter (XR3003, Omega Optical Inc., VT) kept before the optical fiber. The optical fiber was f-number matched to a 0.55 m spectrograph (Jobin-Yovn 550 Triax, Instruments SA, NJ) attached with a liquid nitrogen cooled CCD detector. The spectrograph itself had a computer-controlled adjustable slit and a turret, which held three gratings for a range of measurements. For the Raman studies, a holographic 1800 grooves $mm^{-1}$ grating was used along with the 500 $\mu$m spectrograph entrance slit setting, providing ~4 $cm^{-1}$ resolution. A digital camera (Nikon Coolpix 5400, Nikon, Japan) atop the microscope allowed for registration of the focused laser spot and focusing the image of the laser spot onto the optical fiber. Typically, for Raman studies on liquid samples, a 60× infinity-corrected water immersion objective (Nikon Fluor, Japan, numerical aperture (NA) 1.00) was used. In the case of solid samples, a 60× infinity-corrected objective (Nikon Plan Apo, Japan, NA 0.9) was used. The laser power used at the sample was 6 mW. The typical accumulation time used was 180 s.

**Silver Colloid Preparation and Characterization.** Silver colloids were prepared by the standard Lee and Meisel method.[26] Transmission electron microscopy (TEM) images of Ag were recorded using a JEOL-3010 microscope operating at 300 keV. The TEM images of Ag colloids are shown in Figure 1. The average size of the spherical colloids was found to be ~50 nm.

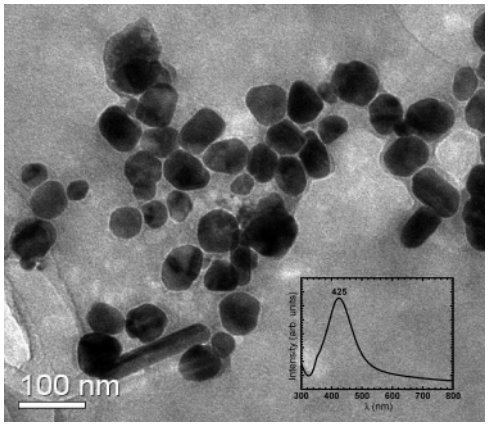


**Figure 1.** TEM image of silver colloids used in the SERS experiments. The inset shows the absorption spectra of silver colloids.

There are some rodlike structures present, whose numbers are negligible when compared to those of the spherical colloidal particles. The inset in Figure 1 shows the extinction spectrum of the Ag colloids, which has the maxima around 425 nm, confirming the expected nature of the Ag colloids.

**SERS of the Aqueous Sample.** p300 solution (protein concentration approximately 40 ng/$\mu$L) was mixed with Ag colloidal solution in the ratio of 1:4 on a glass slide with a cavity in it. After allowing the mixture to settle for 5 min, SERS measurements were performed using the water immersion objective. To find out the effect of chloride ion in the SERS experiments, NaCl solution was mixed with the above suspension in the ratio of 1:10 (NaCl/suspension). The final concentration of NaCl was found to be 0.3 mM in the solution mixture.

**SERS of p300 on a Glass Substrate.** Two methods were used to perform SERS on p300 deposited over the glass substrate. Method I: A 100 $\mu$L solution of Ag colloid was deposited on a flat glass slide and dried overnight at room temperature. A brown-colored ring was observed over which 20 $\mu$L of p300 solution (40 ng/$\mu$L protein in BC100 buffer) was dropped, and the sample was dried at room temperature for 5 h. SERS measurements were performed by focusing the objective onto the uppermost layers of the deposited mixture. Proper care was taken to avoid any contact with the objective while focusing the laser. Method II: A 50 $\mu$L solution of Ag colloid was deposited on a flat glass slide and dried overnight at room temperature. On the ring formed by the colloidal solution, 20 $\mu$L of p300 solution of the same concentration as mentioned above was deposited followed by 50 $\mu$L of Ag colloidal solution. The sample was left to dry at room temperature for 5 h. The SERS measurements were performed as discussed in the method I.

## Results and Discussion

Although p300 is one of the most important multifunctional proteins in humans, very little is known about the structural dynamics of it. However, the structural and functional domain organization of p300 (Figure 2A) indicates that the protein presumably undergoes vibrational reorganization at the amino acid level to achieve diverse functional ability. The functional domains of p300 include nuclear hormone receptor (Nr) cysteine/histidine-rich zinc finger domains CH1 (347−413), CH2 (1195−1451), and CH3 (1669−1807), the KIX domain, the bromo domain (Br), the histone acetyltransferase (HAT) domain, and the minimal HAT domain (1284−1669). The N- and C-terminal domains can act as transactivation domains. As shown in Figure 2B, the recombinant full-length human p300

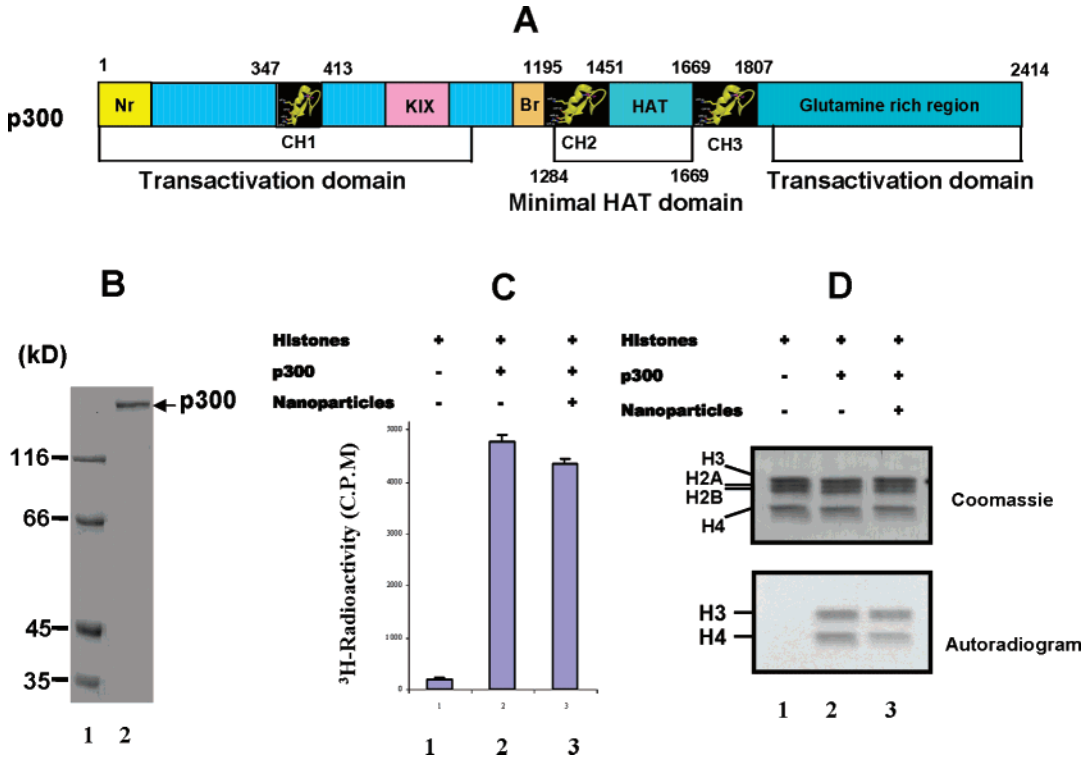


**Figure 2.** (A) Schematic diagram showing the structural and functional domain organization of p300 protein: the functional domains in p300 are indicated, including the nuclear hormone receptor (Nr) cysteine/histidine-rich zinc finger domains CH1 (347−413), CH2 (1195−1451), and CH3 (1669−1807), the KIX domain, the bromo domain (Br), the histone acetyltransferase (HAT) domain, and the minimal HAT domain (1284−1669). The N- and C-terminal domains can act as transactivation domains: 1−2414 represents the amino acids in the protein. (B) Full-length recombinant $His_6$-tagged p300 protein used in the experiment: p300 was purified from recombinant bacculovirus-infected Sf-21 cells and analyzed on 8% SDS−polyacrylamide gel and visualized by coomassie blue staining. Lane 1 is the protein molecular weight marker represented in kDa, and lane 2 is the purified p300 protein. (C) Filter binding assay: HAT assay was performed by using highly purified HeLa core histones (800 ng) in the absence (lane 1) and presence (lane 2) of enzyme p300 (5 ng) and the enzyme (p300) incubated with silver nanoparticles (lane 3). The results represent the average values with error bars (±SD) of three independent experiments. (D) Fluorographic analysis of acetylated histones. HAT assays were performed by using highly purified HeLa core histones (1.2 $\mu$g) in the absence (lane 1) and presence (lane 2) of p300 enzyme (5 ng) and the p300 enzyme incubated with silver nanoparticles (lane 3). The radiolabeled acetylated histones (H3, H2B, H2A, and H4) were resolved on 15% SDS−polyacrylamide gel and visualized by coomassie blue staining and subjected to fluorography followed by autoradiography.

was expressed in Sf-21 insect cell line and purified as described in the Experimental Details. The protein was dialyzed against BC100 buffer to remove imidazole. The HAT activity of p300 was assayed by filter binding and fluorography of radiolabeled acetylated histones (Figure 2, parts C and D). SERS of p300 was carried out with the protein adsorbed on silver nanoparticles. Therefore, it was essential to find out the effect of the silver surface on the functional activity of p300. The HAT activity of p300 incubated with silver nanoparticles was assayed by both filter binding and fluorography. As depicted in Figure 2, parts C and D, the HAT activity of p300 adsorbed on the silver nanoparticle surface remained almost the same as compared to that of the mock incubated enzyme (lane 2 vs 3). These data suggest that the SERS of p300 shown in this report represent the structural dynamics of the functional enzyme.

**SERS Spectra of p300 Protein in the Aqueous Phase.** At first, we took a very high concentration of p300 in solution and carried out a normal Raman experiment. As seen from curve 1 of the inset on the left of Figure 3A, we were unable to see any Raman signature from the p300. If we add silver nanoparticles to this solution, we get very strong Raman signals, which resemble the spectrum shown in curve i of Figure 3A. To determine that these modes are not arising from the nanoparticles or the buffer, we recorded the Raman spectra of the nanoparticles in solution and the SERS of the buffer, separately. In the case of nanoparticles we do not observe any Raman peaks as shown in curve 2 of the inset on the left of Figure 3A. The buffer in the presence of nanoparticles gives strong Raman signals as shown in curve 3 of the inset on the left of Figure 3A. On comparison of this spectrum with the spectrum shown in curve i of Figure 3A, we observe that there are no Raman modes which resemble each other in both the spectra. This suggests that the spectrum in curve i of Figure 3A is indeed coming from the protein p300. Table 1 shows the observed frequencies of the most important Raman bands and their proposed band assignments for the Raman spectrum shown in curve i of Figure 3A. The band assignments have been carried out in accordance with the existing literature pertaining to SERS spectra of amino acids and proteins.[18−20] We describe some of the characteristic SERS vibrations observed in the spectrum. As expected, aromatic rings, amides, and carboxylic group vibrations dominate the SERS spectrum of p300.

*i. Polypeptide Backbone Vibrations.* Figure 3A (curve i) shows three Raman bands associated with the polypeptide backbone at around 1623, 1540, and 1296 $cm^{-1}$. The 1623 $cm^{-1}$ is associated with vibrations of the amide I band. These generally appear in the protein spectra when the α-helix of the protein is in close vicinity of the silver surface. It has been seen that most of the common proteins are adsorbed to the silver surface through the α-helix.[19,20] The next band, viz., 1540 $cm^{-1}$, is due to the amide II vibration. In normal Raman spectra these modes of vibrations are Raman inactive. In the SERS experiments there is a modification in the selection rules giving rise to this band.[14] This is due to the changes in the bond angles, which induce

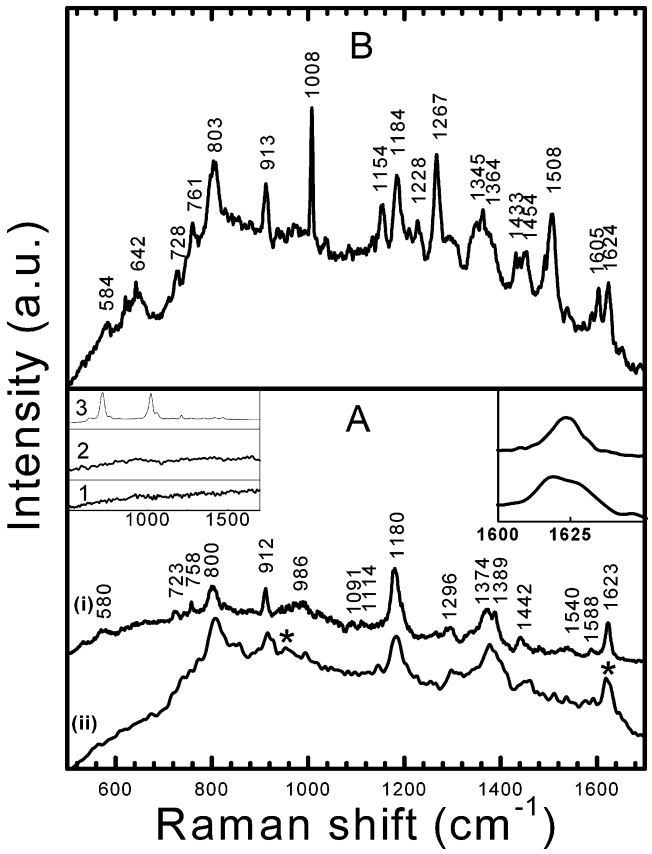


**Figure 3.** (A) Inset on the left shows the Raman spectra of pure p300 solution (curve 1), nanoparticles (curve 2), and buffer with nanoparticles (curve 3). Curve i shows the SERS spectra of p300, and curve ii shows the SERS spectra of deuterated p300. The ∗ has been placed on curve ii to indicate the shifted/new bands in deuterated p300. The inset on the right shows the amide I region for clarity. (B) SERS spectra of p300 in the presence of 0.3 mM NaCl. The concentration of the p300 was ∼40 ng/$\mu$L for all the above cases.

**TABLE 1: Assignment of Raman Bands in the SERS Spectra of p300 Shown in Curve (i) of Figure 3A**[a]

| Raman shift ($cm^{-1}$) | Raman band assignment |
|---|---|
| 1623 | amide I |
| 1588 | $\nu_{as}$ ($COO^-$), His, Trp, and/or Phe ($\nu_{8a}$) |
| 1540 | Trp and/or amide II |
| 1442 | His and/or Trp |
| 1389 | $\nu$ ($COO^-$) |
| 1374 | $\nu$ (CH) |
| 1296 | amide III ($\alpha$-helix) and/or $\delta$ ($CC_\alpha H$) |
| 1180 | Tyr and/or Phe ($\nu_{9a}$) |
| 1114 | $\nu_{as}$ ($C_\alpha CN$) |
| 1091 | $\nu$ ($C_\alpha N$) |
| 912 | $\nu$ ($C-COO^-$) |
| 800 | Tyr and/or $\nu_{as}$ (C−S−C) |
| 758 | Trp or His |
| 723 | $\delta$ $COO^-$) |
| 580 | Trp |

[a] $\nu$, stretching; as, asymmetric; $\delta$, deformation.

changes in the polarizability of the vibrations in the presence of the nanoparticles. However, there are 12 tryptophan (Trp) residues in p300. Therefore, the possibility of this mode overlapping with the Trp cannot be ruled out. The amide III vibration is seen around 1296 $cm^{-1}$. The amide III band often overlaps with the $\delta$ ($CC_\alpha H$) vibrations, and hence the Raman band at 1296 $cm^{-1}$ could have contributions from both of these vibrations.

To confirm these observations, we have performed SERS on deuterated p300. In the deuterated p300, the hydrogens in the amide are replaced by heavy deuteriums. Hence, the vibrational frequencies of the amide bands should decrease in deuterated p300. Curve ii of Figure 3A shows the SERS spectra of deuterated p300. Significantly, curves i and ii of Figure 3A closely resemble each other. Since the deuteration happens only at the amide group, this observation is on the expected lines. Upon deuteration, we observe a decrease in the amide I band frequency by ∼7 $cm^{-1}$. The inset on the right of Figure 3A shows the amide I band region. There is a clear shift from 1623 to 1616 $cm^{-1}$. Since the deuteration is not complete, we do observe a reduced intensity of the 1623 $cm^{-1}$ present in the spectra. In curve ii of Figure 3A, we do observe distinct changes in the regions around 1540 and 1296 $cm^{-1}$. This supports our earlier statement that these peaks are a superposition of the Raman bands of the amide groups and that of other functional groups in the same region. We observe a new mode around ∼950 $cm^{-1}$ in the deuterated p300 spectra (see Figure 3A, curve ii). It is known that upon deuteration the amide III band shifts from 1296 to 950 $cm^{-1}$ (∼340 $cm^{-1}$).[27] These observations confirm the amide band assignments.

It is interesting to note that we do not observe any amide bands pertaining to $\beta$-sheet or random coil of p300 protein. The crystal structures of p300 and CBP (functional twin partner of p300) are not known. The solution structure of the CH1 domain of p300 (32,33), CH3 (34, 35), and KIX (36) domains of CBP reveal that indeed in these domains there is no $\beta$-sheet or random coil. However, on the basis of the primary structure, it could be predicted that p300 may contain very short stretches of $\beta$-sheet as well as random coils. Since none of the structural information available so far is from the full-length protein, our spectral analysis may reflect more realistic structural information about p300. These discrepancies can only be solved by the high-resolution full-length crystal structure of CBP/p300.

*ii. Vibrations Associated with the Aromatic Side Chain.* The SERS spectrum of p300 is dominated by aromatic side chain vibration of tyrosine (Tyr), tryptophan (Trp), and phenylalanine (Phe). Table 1 gives the detailed assignments of these modes. It is necessary to point out here that p300 is quite rich in these aromatic amino acids. There are 12 Trp, 46 Tyr, and 44 Phe present in the primary structure of p300. We do not observe the phenyl ring-breathing mode of Phe as well as the indole ring mode of Trp. This could be due to the fact that these groups may not be in close proximity to the silver surface. This kind of behavior has been observed previously in the SERS spectra of lysozymes adsorbed to silver, where the short-range component of SERS (chemical enhancement) was predominant.[28] It could also be due to the orientation of the molecules with respect to the silver surface. There is a direct implication, of the orientation of the molecule on the silver surface, on the enhancement of the Raman signal.[14]

*iii. Aliphatic Side Chain Vibrations.* The carboxylate group of the aspartic acid (Asp), glutamine (Glu), and/or the C-terminus group in protein interacts with the silver surface to give strong enhancements of these Raman bands.[29] The bands at 1588 and 1389 $cm^{-1}$ are assigned to the asymmetric and symmetric stretching modes of the $COO^-$ group, respectively. In the SERS spectra a strong Raman feature at 912 $cm^{-1}$ is seen, which is due to the $C-COO^-$ stretching. One also observes the Raman band at 723 $cm^{-1}$ due to $\delta(COO^-)$ vibrations. There are two weak bands around 1091 and 1114 $cm^{-1}$, which are due to the symmetric stretching of ($C_\alpha N$) and the asymmetric stretching of ($CC_\alpha N$) groups, respectively. This observation suggests that the p300 adsorbs to the silver nanoparticles through the nitrogen groups. This could be one

**TABLE 2: Assignment of Raman Bands in the SERS Spectra of p300 + 0.3 mM NaCl Shown in Figure 3B**

| Raman shift ($cm^{-1}$) | Raman band assignment |
|---|---|
| 1624 | amide I |
| 1605 | Trp, Tyr, and/or Phe ($\nu_{8a}$) |
| 1508 | His |
| 1454 | $\delta$ ($CH_2$) |
| 1433 | His and/or Trp |
| 1364 | Trp |
| 1345 | $\delta$ (CH) and/or Trp |
| 1267 | $\nu$ (C═O) ($\alpha$-helix) |
| 1184 | Tyr and Phe |
| 1153 | $\nu$ (C−N) |
| 1008 | Phe ($\nu_{12}$) |
| 913 | $\nu$ (C−$COO^-$) |
| 803 | Tyr |
| 761 | Trp or His |
| 728 | $\delta$ $COO^-$) |
| 642 | Tyr |
| 584 | Trp |

of the reasons for the presence of strong amide bands in the SERS of p300.

**SERS Spectra of p300 Protein in the Presence of Colloidal Aggregating Agent.** Although the role of aggregating agents in SERS has been studied earlier with respect to small molecules,[30,31] proteins are yet to be investigated in great detail. Upon addition of a small quantity of NaCl or KCl to the solution containing the analyte and nanoparticles, one observes a large enhancement in the SERS signal. As it is known, the enhancement of Raman bands in SERS is governed by both electromagnetic enhancement and the chemical enhancement.[14] Upon addition of small concentrations of $Cl^-$ ions to the protein−nanoparticle composite there is an aggregation of nanoparticles around the protein molecule. This will cause a further enhancement in the above-mentioned mechanisms due to (i) an enhanced plasmon coupling as a result of the aggregation of the nanoparticles, (ii) an increased charge-transfer pathway between the metal−protein system, and (iii) the anion-induced reorientation of adsorbed protein.[30] These will not only account for the enhanced Raman signal intensity but also for the appearance of new modes of vibrations upon the addition of $Cl^-$ ions in the solution.

Figure 3B shows the SERS spectrum of p300 in the presence of 0.3 mM NaCl. Table 2 shows the frequencies of the most important SERS bands and their proposed band assignments. We observe new modes of vibrations arising upon the addition of $Cl^-$ ions (see Figure 3B). We can clearly see new Raman bands around 1008, 1267, 1508, and 1605 $cm^{-1}$, which have been assigned to the groups Phe, C═O stretching of the $\alpha$-helix, histidine (His)/Trp, and Tyr and/or Phe, respectively. Note that p300 contains 68 His residues along with several Trp, Tyr, and Phe as mentioned earlier; hence, the SERS spectra of p300 reported in this paper are realistic. Predicted structural data[32−36] also suggest the presence of stretches of the $\alpha$-helix throughout the p300 structure. It is to be noted that there is a strong resemblance in the spectra with and without $Cl^-$ ion as shown in Figure 3, parts A and B. This suggests that the $Cl^-$ ion effect could be used in the studies of proteins using SERS.

**SERS Spectra of p300 Adsorbed to Silver Nanoparticles Dried over a Glass Substrate.** The SERS spectra of p300 obtained by method I (see the Experimental Details) is shown in Figure 4A. Enhanced Raman signals for the bands around 634, 721, 1013, and 1268 $cm^{-1}$ are observed. These bands are stretching vibrations of Phe and C═O and are absent in SERS spectra of p300 recorded in the aqueous solution (compare with Figure 3A). It is important to note the absence of the amide vibration in Figure 4A. The absence of amide bands could be due to the fact that these groups are not in the close proximity to silver surface, since the silver collides are immobilized on the glass slides apriori. This also could be due to screening of the amide groups by the aromatic groups on the protein surface.[27] In the absence of a short-range component of the SERS mechanism, the amide bands can disappear in the SERS spectra.

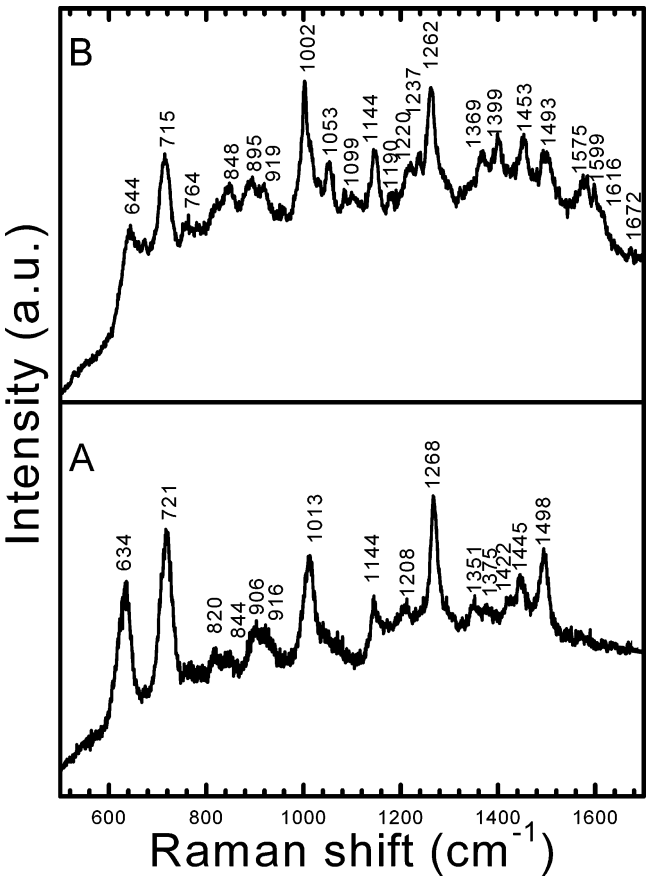


**Figure 4.** SERS spectra of p300 in the nonaqueous form on substrates prepared by (A) method I and (B) method II (the Experimental Details gives the details of the substrate preparation). The concentration of the p300 was again ~40 ng/$\mu$L.

SERS spectra were also obtained by preparing the sample using method II (see the Experimental Details), which we call the "sandwich technique". Figure 4B shows the SERS spectra of p300 obtained by method II. Here, we observe a weak amide I band around 1672 $cm^{-1}$ along with many other modes, which were absent in the SERS spectra obtained by method I. It is interesting to observe that the Raman spectrum of p300 prepared by the "sandwich technique" (Figure 4B) resembles the Raman spectrum of the p300 in aqueous solution in the presence of chloride ion (Figure 3B). Since, in the "sandwich" case, we add the nanoparticles along with the protein on top of a dried silver nanoparticle layer, this allows a better adsorption of the protein to the silver surface and provides an environment to retain minute amounts of water between the silver nanoparticles. Although the enhancement of the Raman signal obtained by this method is less when compared to that of the spectra obtained in aqueous form, this technique may still facilitate a unique opportunity to perform SERS studies in "chemically pure" conditions, especially under ultrahigh vacuum conditions.

## Conclusions

For the first time, SERS was performed on p300 in aqueous and dry forms. The SERS spectra suggest the presence of

α-helix, aromatic ring structures like Phe, Tyr, Trp, His, and aliphatic structures such as Asp, Glu, and C-terminus groups in p300. The presence of these Raman bands in the SERS of the protein provides an important tool for studying drug−protein interactions. In the absence of full-length crystallographic data of proteins, SERS could provide a very useful technique to obtain structural information. The presence of small concentrations of NaCl leads to aggregation of nanoparticles leading to a better adsorption of silver nanoparticles to the proteins. The chloride ion could increase the sensitivity of SERS experiments due to larger enhancement in Raman signals more or less retaining the Raman spectra of the proteins. In this paper, we demonstrate a new method called the "sandwich technique", which could provide an alternate method for recording SERS spectra of proteins without the aqueous medium. In the present case, we were able to record the Raman spectra of p300, which resembles its spectra in the aqueous medium. This method could pave the way to perform SERS experiments in ultrahigh vacuum conditions. Furthermore, SERS analysis can be used to study protein−ligand interactions, like p300−HAT modulator interaction, which would have immense implications in drug design.

**Acknowledgment.** T.K.K. thanks the Department of Biotechnology, Government of India for the financial support for this work. M.A. thanks CSIR for his Junior Research fellowship. C.N. thanks Professor M. R. S. Rao and JNCASR for funding the Raman work through an Inter-departmental collaborative project.

## References and Notes

(1) Eckner, R.; Ewen, M. E.; Newsome, D.; Gerdes, M.; DeCaprio, J. A.; Lawrence, J. B.; Livingston, D. M. *Genes Dev.* **1994**, *8*, 869.
(2) Giles, R. H.; Peters, D. J.; Breuning, M. H. *Trends Genet.* **1998**, *14*, 178.
(3) Giordano, A.; Avantaggiati, M. L. *J. Cell. Physiol.* **1999**, *181*, 218.
(4) Goodman, R. H.; Smolik, S. *Genes Dev.* **2000**, *14*, 1553.
(5) Chan, H. M.; La Thangue, N. B. *J. Cell Sci.* **2001**, *114*, 2363.
(6) Iyer, N. G.; Ozdag, H.; Caldas, C. *Oncogene* **2004**, *23*, 4225.
(7) Bannister, A. J.; Kouzarides, T. *Nature* **1996**, *384*, 641.
(8) Ogryzko, V. V.; Schiltz, R. L.; Russanova, V.; Howard, B. H.; Nakatani, T. *Cell* **1996**, *87*, 1107.
(9) Das, C.; Kundu, T. K. *IUBMB Life* **2005**, *57*, 137.
(10) Swaminathan, V.; Kishore, A. H.; Febitha, K. K.; Kundu, T. K. *Mol. Cell. Biol.* **2005**, *25*, 7534.
(11) Varier, R. A.; Swaminathan, V.; Balasubramanyam, K.; Kundu, T. K. *Biochem. Pharmacol.* **2004**, *68*, 1215.
(12) Fleischman, M.; Hendra, P. J.; McQuillan, A. J. *Chem. Phys. Lett.* **1974**, *26*, 163.
(13) Kneipp, K.; Kneipp, H.; Itzkan, I.; Dasari, R. R.; Feld, M. S. *J. Phys.: Condens. Matter* **2002**, *14*, R597.
(14) Moskovits, M. *Rev. Mod. Phys.* **1985**, *57*, 783.
(15) Jing, N.; Lipert, R. J.; Dawson, G. B.; Porter, M. D. *Anal. Chem.* **1999**, *71*, 4903.
(16) Graham, D.; Mallinder, B. J.; Smith, W. E. *Angew. Chem., Int. Ed.* **2000**, *39*, 1061.
(17) Moore, B. D.; Stevenson, L.; Watt, A.; Flitsch, S.; Turner, N. J.; Cassidy, C.; Graham, D. *Nat. Biotechnol.* **2004**, *22*, 1133.
(18) Podstawka, E.; Ozaki, Y.; Lroniewicz, L. M. *Appl. Spectrosc.* **2004**, *58*, 570.
(19) Stewart, S. P.; Fredericks, M. *Spectrochim. Acta, Part A* **1999**, *55*, 1615.
(20) Podstawka, E.; Ozaki, Y.; Lroniewicz, L. M. *Appl. Spectrosc.* **2004**, *58*, 1147.
(21) Fabriciova, G.; Cortes, S. S.; Ramos, J. V. C.; Miskovsky, P. *Biopolymers* **2004**, *74*, 125.
(22) Ermishov, M.; Sukhanova, A.; Kryukov, E.; Grokhovsky, S.; Zhuze, A.; Oleinikov, V.; Jardillier, J. C.; Nabiev, I. *Biopolymers* **2000**, *57*, 272.
(23) Streltsov, S.; Oleinikov, V.; Ermishov, M.; Mochalov, K.; Sukhanova, A.; Nechipurenko, Y.; Grokhovsky, S.; Zhuze, A.; Pluot, M.; Nabiev, I. *Biopolymers* **2003**, *72*, 442.
(24) Kundu, T. K.; Wang, Z.; Roeder, R. G. *Mol. Cell. Biol.* **1999**, *19*, 1605.
(25) Balasubramanyam, K.; Swaminathan, V.; Ranganathan, A.; Kundu, T. K. *J. Biol. Chem.* **2003**, *278*, 19134.
(26) Lee, P. C.; Meisel, D. *J. Phys. Chem.* **1982**, *86*, 3391.
(27) Tuma, R.; Prevelige, P. E., Jr.; Thomas, G. J., Jr. *Proc. Natl. Acad. Sci. U.S.A.* **1998**, *95*, 9885.
(28) Chumanov, G. D.; Efremov, R. G.; Nabiev, I. R. *J. Raman Spectrosc.* **1990**, *21*, 43.
(29) Grabbe, E. S.; Buck, R. P. *J. Am. Chem. Soc.* **1989**, *111*, 8362.
(30) Li, Y. S.; Wang, Y.; Cheng, J. *Vib. Spectrosc.* **2001**, *27*, 65.
(31) Flauds, K.; Littlewood, R. E.; Graham, D.; Dent, G.; Smith, W. E. *Anal. Chem.* **2004**, *76*, 592.
(32) Freedman, S. J.; Sun, Z. Y.; Poy, F.; Kung, A. L.; Livingston, D. M.; Wagner, G.; Eck, M. J. *Proc. Natl. Acad. Sci. U.S.A.* **2002**, *99*, 5367.
(33) Dial, R.; Sun, Z. Y.; Freedman, S. J. *Biochemistry* **2003**, *42*, 9937.
(34) De Guzman, R. N.; Liu, H. Y.; Martinez-Yamout, M.; Dyson, H. J.; Wright, P. E. *J. Mol. Biol.* **2000**, *303*, 243.
(35) Legge, G. B.; Martinez-Yamout, M. A.; Hambly, D. M.; Trinh, T.; Lee, B. M.; Dyson, H. J.; Wright, P. E. *J. Mol. Biol.* **2004**, *343*, 1081.
(36) Radhakrishnan, I.; Perez-Alvarado, G. C.; Parker, D.; Dyson, H. J.; Montminy, M. R.; Wright, P. E. *Cell* **1997**, *91*, 741.